HHS Public Access

Author manuscript

Am J Ophthalmol. Author manuscript; available in PMC 2024 September 01.

Published in final edited form as:

Am J Ophthalmol. 2023 September ; 253: 1–11. doi:10.1016/j.ajo.2023.04.011.

Decreased Central Macular Choriocapillaris Perfusion Correlates with Increased Low Luminance Visual Acuity Deficits

Mengxi Shen[1], **Jianqing Li**[1], **Yingying Shi**[1], **Qinqin Zhang**[2], **Ziyu Liu**[3], **Hao Zhou**[3], **Jie Lu**[3], **Yuxuan Cheng**[3], **Zhongdi Chu**[3], **Xiao Zhou**[3], **Jeremy Liu**[1], **Xiaoshuang Jiang**[1], **Liang Wang**[1], **Rita Laiginhas**[1], **Luis de Sisternes**[2], **Elizabeth A. Vanner**[1], **William J. Feuer**[1], **Ruikang K. Wang**[3,4], **Giovanni Gregori**[1], **Philip J. Rosenfeld**[1]

[1]Department of Ophthalmology, Bascom Palmer Eye Institute, University of Miami Miller School of Medicine, Miami, Florida, USA

[2]Research and Development, Carl Zeiss Meditec, Inc., Dublin, CA, USA

[3]Department of Bioengineering, University of Washington, Seattle, Washington, USA

[4]Department of Ophthalmology, University of Washington, Seattle, Washington, USA

Abstract

Purpose: Correlations between low luminance visual acuity deficits (LLVADs) and central choriocapillaris perfusion deficits were investigated to help explain how increases in LLVAD scores at baseline predict annual growth rates of geographic atrophy (GA).

Design: Prospective cross-sectional study.

Methods: Photopic luminance best-corrected visual acuity (PL-BCVA) and low luminance BCVA (LL-BCVA) were measured using the Early Treatment Diabetic Retinopathy Study chart. LL-BCVA was measured using a 2.0-log unit neutral density filter. LLVADs were calculated as the difference between PL-BCVA and LL-BCVA. Within a fovea-centered 1mm circle, the percentage of choriocapillaris flow deficits (CC FD%), drusen volume, optical attenuation coefficient (OAC) elevation volume, and the outer retinal layer (ORL) thickness were assessed.

Results: In all 90 eyes (30 normal eyes; 31 drusen-only eyes; 29 non-foveal GA eyes), significant correlations were found between the central CC FD% and PL-BCVA ($r=-0.393$, $p<0.001$), LL-BCVA ($r=-0.534$, $p<0.001$), and the LLVAD ($r=0.439$, $p<0.001$). Central cube root (cubrt) drusen volume, cubrt OAC elevation volume, and ORL thickness were correlated with PL-BCVA, LL-BCVA and LLVADs (all $p<0.05$). Stepwise regression models showed that central cubrt OAC elevation volume and ORL thickness were associated with PL-BCVA ($R^2=0.24$, $p<0.05$); central CC FD%, cubrt OAC elevation volume, and ORL thickness were associated with

Corresponding Author Philip J. Rosenfeld, MD, PhD, Bascom Palmer Eye Institute, 900 NW 17th street, Miami, FL, 33136, Voice: 305-326-6148, Fax: 305-326-6538, prosenfeld@miami.edu.

LL-BCVA (R^2=0.44, p<0.01); and central CC FD% and ORL thickness were associated with LLVAD (R^2=0.24, p<0.01).

Conclusions: The significant correlations between central CC FD% and LLVAD support the hypothesis that the ability of LLVAD to predict the growth of GA is mediated through a decrease in macular choriocapillaris perfusion.

Table of Contents

Diminished low luminance visual function is shown to correlate with decreased choriocapillaris perfusion within the central macula. Previously, both decreased choriocapillaris perfusion and increased low luminance visual acuity deficits were shown to correlate with increased growth rates of geographic atrophy. This report supports our previous hypothesis that both decreased low luminance visual function and increased growth rates of geographic atrophy are mediated through the same underlying decrease in central macular choriocapillaris perfusion.

Keywords

Photopic luminance visual acuity; low luminance visual acuity; low luminance visual acuity deficit; choriocapillaris; flow deficits; pseudophakia; swept-source; optical coherence tomography angiography; outer retinal layer; drusen; geographic atrophy; choroidal hypertransmission defects

INTRODUCTION

Photopic luminance (PL) and low luminance (LL) best-corrected visual acuity (BCVA) are visual function measurements that rely primarily on central cone photoreceptors and are measured using a standard Early Treatment for Diabetic Retinopathy Study (ETDRS) chart.[1] LL-BCVA is measured by placing a 2.0-log unit neutral density filter in front of the eye, which lowers the ambient luminance 100-fold. LL-BCVA measurements are performed immediately after PL-BCVA measurements by placing the neutral density filter in front of the eye without allowing time for dark adaptation.[2] Sunness *et al.*[2,3] were the first to use LL-BCVA testing in eyes with nonexudative age-related macular degeneration (neAMD). In their study, they sequentially performed PL-BCVA and LL-BCVA testing in subjects with geographic atrophy (GA) secondary to neAMD. The low luminance visual acuity deficit (LLVAD) measurement was calculated by subtracting the LL-BCVA letter score from the PL-BCVA letter score. They found that in eyes with 20/50 or better PL-BCVA at baseline, this LLVAD measurement predicted a 3-line loss of vision in two years. Our proposed explanation for how the LLVAD measurement might predict future vision loss was that it predicts the growth rate of GA, since faster growing lesions would have a greater chance of involving the fovea and therefore affecting the vision.[4] To test our hypothesis, we studied the relationship between the LLVAD measurements and the growth rate of GA lesions in the Complement Inhibition with Eculizumab for the Treatment of Non-Exudative Macular Degeneration (COMPLETE) Study, a randomized, double-arm, double-masked phase 2 study.[4] We found that the LLVAD measurements at baseline predicted GA growth rates during the next 6 months and this finding was confirmed at 12 months of follow-up. Since our report, at least five prospective clinical trials have confirmed the power of baseline LLVAD measurements in predicting subsequent annual growth rates of GA.[5–11]

Another baseline predictor of the annual GA growth rates is the loss of choriocapillaris (CC) perfusion throughout the macula, measured as an increase in CC flow deficits (FDs).[12] While CC FDs were shown to be highest in the region closest to the margin of GA and this region correlated with GA growth rates, we also have found significant and similar correlations between GA growth rates and increased CC FDs away from the margins of GA and throughout the 6X6 mm scan area.[12] These findings suggested to us a possible explanation for why the decrease in LLVAD measurements, a foveal cone photoreceptor function, might be associated with more rapid growth rates of GA, even when the lesions may not be adjacent to the foveal region.[4] We proposed that this effect at a distance could be explained if the increase in central LLVAD measurements also correlated with a decrease in central CC perfusion. A correlation between LLVAD and CCFD measurements might explain the correlation between LLVAD and GA growth rates. More importantly, since increases in LLVAD measurements appear even before the PL-BCVA is affected,[13] the measurement of LLVADs could serve as a surrogate marker for increases in CC FDs and possibly other structural changes in the macula that could impact foveal LL visual function in eyes with neAMD.

To test if the central foveal PL-BCVA, LL-BCVA, and LLVAD scores correlated with central CC FD and other macular structural characteristics, we designed a prospective, observational study known as the Comparison of Low Luminance Visual Acuity Testing Before and After Cataract Surgery (COMPARE) study. This study consisted of two parts. The first part investigated the impact of cataracts on PL-BCVA, LL-BCVA, and LLVAD scores by measuring these scores before and after cataract surgery.[14] This first step was necessary to elucidate whether cataracts influenced LLVAD measurements before we attempted to correlate LLVAD with CC FD measurements. We found that the LLVAD scores were not reproducible in the same eye before and after cataract surgery. We concluded that the presence of cataracts had an unpredictable impact on LL-BCVA measurements compared with PL-BCVA measurements. Since we wanted to correlate the LLVAD with central macular structural parameters and the magnitude of the LLVAD measurements from phakic eyes depended on the type and severity of the cataract, we decided to restrict this analysis to pseudophakic eyes.

The current report is from the second part of the COMPARE study in which we investigated the relationship between PL-BCVA, LL-BCVA, and LLVAD scores with the central 1 mm CC FD measurements to determine if the function of these central cone photoreceptors correlated with CC FDs in pseudophakic normal eyes and pseudophakic eyes with neAMD. We also included additional parameters that could be extracted from the same swept-source optical coherence tomography (SS-OCT) scans. These included the central drusen volume,[15] central optical attenuation coefficient (OAC) elevation volume,[16] and central outer retinal layer (ORL) thickness.[17]

METHODS

The prospective COMPARE study was approved by the institutional review board of the University of Miami Miller School of Medicine. Informed consent was obtained from all participants. The study was performed in accordance with the tenets of the Declaration

of Helsinki and complied with the Health Insurance Portability and Accountability Act of 1996. The first part of the COMPARE study evaluated the effect of cataract surgery on PL-BCVA, LL-BCVA- and LLVAD scores,[14] while the second part of the COMPARE study focused on the pseudophakic eyes and studied the correlations of BCVA and LLVAD scores with central CC FD measurements as well as other anatomic measurements including drusen volume,[15] OAC elevation volume,[16] and ORL thickness.[17]

Patients with normal eyes and neAMD eyes were recruited from retinal service and cataract service at the Bascom Palmer Eye Institute. Both normal eyes and eyes with neAMD were required to have a PL-BCVA letter score of ≥ 64 (Snellen equivalent of 20/50 or better). Subjects with normal eyes had no history of ocular disease and no evidence of optic disc, retinal, or choroidal pathology on clinical fundus biomicroscopic examination and OCT imaging. Exclusion criteria for all eyes included an axial length ≤ 23 mm or ≥ 26 mm. Eyes with either intermediate and late stage neAMD were included, but eyes with a previous history of exudation or any prior treatment were excluded. Eyes with intermediate neAMD were diagnosed as having at least one druse with a diameter ≥ 125 μm observed on fundus biomicroscopy or color fundus photography and confirmed on SS-OCT imaging. Eyes with late neAMD were defined as having a history or presence of drusen with evidence of macular atrophy characterized by persistent choroidal hypertransmission defects (hyperTDs) defined as having a greatest linear dimension ≥ 250 μm as measured using *en face* images from a slab corresponding to segmentation boundaries extending 64 μm to 400 μm beneath Bruch's membrane (BM).[18–20] Only eyes with non-foveal involving persistent choroidal hyperTDs as determined by SS-OCT B-scan localization of the fovea were included. Since the CC FDs were measured within a 1 mm circle centered on the fovea, the posterior margin of atrophy could not involve the foveal center, and the area of atrophy together with any hyperpigmentation could not comprise more than 20% of a central 1 mm circle centered on the fovea.

All eyes underwent SS-OCT imaging (PLEX® Elite 9000, Carl Zeiss Meditec, Inc. Dublin, CA). The SS-OCT instrument has a laser light source with a central wavelength of 1050 nm, a bandwidth of 100 nm, and an axial resolution in tissue of approximately 5 μm with a transverse resolution at the retinal surface of approximately 20 μm. The instrument operated at a scanning speed of 100,000 A-scans per second. All patients were imaged using the SS-OCT angiography (SS-OCTA) 6×6 mm scan pattern centered on the fovea. This scan pattern consists of 500 A-scans per B-scan, with each B-scan repeated twice at each position to generate the angiographic flow signal, and 500 B-scan positions along the slow y-axis, resulting in a uniform spacing of 12 μm between A-scans. Each A-scan had a depth of 3 mm consisting of 1536 pixels per A-scan. The angiographic flow information was obtained using the complex optical microangiographic algorithm known as OMAG^{C} that generates the flow signals from the variations in both the OCT signal magnitude and phase information between sequential B-scans acquired at the same position.[21,22] Four individual 6×6 mm scans were acquired for each study eye in each imaging session. Scans with a signal strength less than 7 based on the instrument's output, as well as scans with significant motion artifacts, were excluded.

In addition to using signal strength, scans were assessed using a novel OCTA quality map algorithm to minimize the variations and to ensure the reliability of these measurements since all the parameters were measured in the central 1 mm circle.[23] This proprietary image quality algorithm, available on the Advanced Retinal Imaging Network website (Carl Zeiss Meditec, Inc. Dublin, CA), measured textural features extracted from the flow and structural slabs obtained from the SS-OCTA scan volume in order to provide a quantification of image quality for the angiography component of the acquisition. Four different *en face* slabs (1 for maximum flow information and 3 for average, maximum and minimum intensity properties, respectively) were generated from each scan volume restricting the *en face* projection of the retina from the ILM to the RPE and processed to generate 88 Haralick feature maps (22 maps from each independent slab). Each of these feature maps provide a pixel-by-pixel representation of the statistical and textural properties of the analyzed image within a small neighborhood and are commonly used in the machine learning literature.[24] Since the extracted features describe intrinsic characteristics of the images, no resizing was done for any of the slabs or feature maps, keeping the original size of 500×500 pixels for a 6×6 mm *en face* field of view. A machine learning algorithm was then trained to use these features to match quality maps drawn by expert annotators in a pixel-by-pixel manner. Training of the algorithm was conducted in a set of images outlined by graders in terms of quality (5-scale of increasing quality gradings, which were drawn directly pixel-by-pixel in the *en face* images) where five independent graders evaluated the same given images All graders received the necessary training with specific instructions to judge the quality of given OCT-A regions using the 5-scale.

In the expert quality annotations, poor image quality was generally due to a combination of four factors: 1) poor signal level, 2) high noise 3) poor resolution, and 4) significant motion artifacts. The ground truth training target for a supervised machine learning model was established as the average quality map resulting from these 5 graders. Lasso regression (a linear regression model where each feature map receives a weight to account for computed quality) was then used to generate a linear model matching the feature map values to the ground truth drawn by the graders in a pixel-by-pixel manner.[25] Although further details about this method remain undisclosed because this OCTA quality map algorithm is part of the software present in the instrument's latest commercial release, its performance has passed the quality standards established by the device's manufacturer when tested in a set of independent images from the training set against pixel-by-pixel outlined quality annotations by a different set of graders. This quality map is used to judge the quality of an individual scan across the field of view, to quantify the difference in quality among several acquisitions of the same subject, and to provide an overall quality metric of a single acquisition by averaging the map values in a region of interest. These quality measurements ranged from a value of 1 (clinically unusable) to 5 (excellent quality). We used a threshold of 2.5 as the cutoff, and there was no tolerance for any low-quality area within the central 1 mm circle. Three out of four 6X6 mm scans with the best image quality scores from each eye were chosen for further analysis.

Both PL-BCVA and LL-BCVA tests were performed according to the standard ETDRS protocol using standard back illuminated ETDRS charts at 4 meters. The PL-BCVA and LL-BCVA score were recorded in number of letters. With the room lights off, these back

illuminated ETDRS charts had a surface luminance level of 160 cd/m^2 at the center of the chart. We first performed standard PL-BCVA measurements for both eyes, using Chart 1 for the right eye and then Chart 2 for the left eye. The LL-BCVA measurements were obtained immediately after the PL-BCVA measurements by inserting a 2.0-log unit neutral density filter in front of the lenses in the trial frame for each eye. This neutral density filter decreased the ambient luminance 100-fold (Wratten filter; Kodak, Rochester, NY). We then tested LL-BCVA for both eyes, using Chart 1 for the right eye and then Chart 2 for the left eye. Of note, the LL-BCVA testing is a mesopic measurement that does not require dark adaptation. The LLVAD was then calculated by subtracting the LL-BCVA ETDRS letter score from the PL-BCVA ETDRS letter score as previously described.[2,4,26]

Visualization and quantitation of the CC were performed using the 6×6 mm scans to compute the CC FD percentage (CC FD%) within a central 1 mm circle centered on the fovea. The CC measurements were obtained using a 16 μm thick slab with its anterior boundary located 4 μm beneath the Bruch's membrane (BM).[27] The corresponding *en face* structural slabs (Figure 1, B, F, J) were used to compensate for any signal loss due to the overlying anatomy, and retinal vessel projection artifacts were removed from the CC slab.[28–30] CC FD% measurements were obtained from the compensated CC *en face* flow images (Figure 1, C, G, K) after excluding any areas with hyperpigmentation[31] and hyperTDs.[20] The CC FDs were then quantified using the fuzzy C-means algorithm (FCM method) as previously described.[32,33] CC FD% was defined as the ratio of FD area to the total quantifiable area within a 1 mm circle (Figure 1, D, H, L).

The drusen volume measurements were generated using a validated algorithm known as the Advanced RPE Analysis Algorithm version 0.10 available on the Advanced Retinal Imaging Network website (Carl Zeiss Meditec, Inc. Dublin, CA).[15] Drusen volumes were obtained in the 1 mm and 3 mm circles centered at the fovea.

Algorithms based on OAC OCT imaging were used to measure the ORL thickness[17] and the elevation of the RPE relative to BM, which is referred to as the OAC elevation volume.[16] As previously described, the ORL was defined as extending from the upper boundary of the OPL to the RPE layer.[17] The OAC elevation volume (Figure 2, B, E, H) and the ORL thickness measurements (Figure 2, C, F, I) in the central 1 mm circle were obtained after excluding the areas of hyperpigmentation and hyperTDs.

All the above-mentioned measurements, including the CC FD%, drusen volume, OAC elevation volume, and ORL thickness in the central 1 mm circle, were measured from three repeated scans with acceptable image quality within the central 1 mm circle and the values were averaged for further statistical analyses. Statistical analyses were performed using the IBM Statistical Package for the Social Sciences (SPSS) software version 27 (IBM Corporation, Armonk, NY) with a p-value of < 0.05 considered to be statistically significant. Descriptive statistics for continuous variables include means and standard deviations. Pearson correlation was used to determine the correlations of PL-BCVA, LL-BCVA and LLVAD with age, central CC FD%, central cube root (cubrt) drusen volume, central cubrt OAC elevation volume, and central ORL thickness. Stepwise regression was performed to determine which of the characteristics contributed to the PL-BCVA, LL-BCVA and

LLVAD scores. A sensitivity analysis was performed on the final model of each stepwise regression using generalized estimating equations (GEE) with exchangeable correlation structure used to account for the inclusion of two eyes of some subjects. The cubrt OAC elevation volumes in the 1 mm circle were used in the regression model in lieu of the drusen volume measurements since the OAC elevation volume was highly correlated with the drusen volume and was a more sensitive measure of basal laminar deposits,[16] so including both would be redundant.

RESULTS

A total of 90 pseudophakic eyes from 63 subjects with and without neAMD were enrolled between August 2018 and March 2022. Among these 90 eyes, there were 30 normal eyes, 31 drusen-only eyes, and 29 non-foveal GA (nfGA) eyes. The average age was 74.17±8.43 years and 66% were female. The mean scores of PL-BCVA, LL-BCVA, and LLVAD were 83.27±7.02, 69.69±10.29 and 13.58±6.22 letters, respectively.

The mean CC FD% in the central 1 mm circle was 14.36%±7.91%. The mean ORL thickness measurement in the central 1 mm circle was 184.70±21.88 μm. The mean cubrt drusen volume and mean cubrt OAC elevation in the 1 mm circle are 0.13±0.15 mm and 0.21±0.13 mm, respectively. The values for all three subgroups are shown in Table 1. Among the three subgroups of normal, drusen-only, and nfGA eyes, there were significant differences in age and PL-BCVA, LL-BCVA, and LLVAD scores. Within the central 1 mm circle, there were significant differences in the CC FD%, cubrt drusen volume, cubrt OAC elevation volume, and ORL thickness measurements. Not surprisingly, there was also a difference in the cubrt drusen volume within the central 3 mm circle among three subgroups, but this parameter was not included in the stepwise regressions (below) due to concerns about multicollinearity among predictors.

Age was found to significantly correlate with PL-BCVA, LL-BCVA, and LLVAD scores among all the 90 eyes (Table 2, all $p \leq 0.002$). Within the central 1 mm circle, CC FD%, cubrt drusen volume, cubrt OAC elevation volume, and ORL thickness were significantly correlated with PL-BCVA, LL-BCVA, and LLVAD (Table 2, all $p \leq 0.028$). Figure 3 depicts the significant correlations between the CC FD% in central 1 mm circle with PL-BCVA ($r = -0.393$, $p < 0.001$), LL-BCVA ($r = -0.534$, $p < 0.001$), and LLVAD ($r = 0.439$, $p < 0.001$), respectively. All these analyses were performed using the entire sample of 90 eyes.

Stepwise regression models (Table 3) revealed that for the PL-BCVA measurements, the cubrt OAC elevation volume ($p < 0.001$) and the ORL thickness ($p = 0.016$) within the central 1 mm circle were included in the final model ($R^2 = 0.24$). For the LL-BCVA measurements, the cubrt OAC elevation volume ($p < 0.001$), the ORL thickness ($p = 0.004$), and the CC FD% ($p = 0.009$) within the central 1 mm circle were included in the final model ($R^2 = 0.44$). For the LLVAD measurements, the CC FD% ($p = 0.007$) and the ORL thickness ($p = 0.007$) within the central 1 mm circle were included in the final model ($R^2 = 0.24$). In all the regression models, the residuals were normally distributed. While age, the CC FD% in central 1 mm circle, cubrt OAC elevation volume in the central 1 mm circle, and ORL thickness in the central 1 mm circle were all significantly correlated with each

other, the stepwise regression model only included the parameters that were independently, significantly correlated with the PL-BCVA, LL-BCVA and LLVAD scores, while avoiding multicollinearity among significantly correlated predictors. The sensitivity analyses with the GEE models produced similar results as the stepwise regressions.

The predicted values for the PL-BCVA, LL-BCVA and LLVAD scores obtained from the stepwise regression models were compared with the observed values of PL-BCVA, LL-BCVA and LLVAD scores. As shown in Figure 4, there were significant correlations between the predicted and the observed values of PL-BCVA ($r= 0.506$, $p<0.001$), LL-BCVA ($r= 0.677$, $p<0.001$) and LLVAD scores ($r= 0.507$, $p<0.001$).

DISCUSSION

In this study, we showed a correlation between low luminance visual acuity measurements and choriocapillaris perfusion within the central macula. This correlation between the central 1 mm CC FD% and the LLVAD measurements supports our proposed hypothesis that the link between LLVAD measurements and the increased growth rate of GA could be explained by the decrease in CC perfusion in eyes with neAMD.[4] This relationship would explain how a foveal visual function test, such as the LL-BCVA test, could be correlated with the growth of GA that is away from the central fovea. Of note, we also showed a correlation between LLVAD measurements and the ORL thickness in the central macula, which is not surprising given the fact that the LLVAD measurements should correspond primarily to cone photoreceptor health, which corresponds to the central ORL thickness.[34] Together, both the CC FD% and the ORL thickness served as the parameters that could be used to predict the LLVAD measurements (Table 3).

While we are unaware of any studies that investigated the relationship between the central ORL thickness and the growth rate of GA in eyes with nfGA, it would not be surprising if such a relationship exists given the reports of photoreceptor damage around the margins of GA.[35–37] While the cause and effect relationship cannot be established by this study, it is tempting to speculate that the underlying CC perfusion deficits are responsible for both the ORL thinning and the increase in LLVAD measurements; however, we cannot rule out the possibility that it is the thinning of the ORL, perhaps along with RPE dysfunction, that drives the loss of CC perfusion.

Since our prior study showed that the LLVAD scores were predictive of GA growth rates while PL-BCVA and LL-BCVA scores were not predictive of GA growth rates,[4] we would have expected the stepwise multiple regression models to identify macular parameters other than CC FD% that contributed to these different visual function measurements. For PL-BCVA, we found that the OAC elevation volume, which was highly correlated with drusen volume, and the ORL thickness were retained in the final prediction model. This is consistent with our observations that photoreceptors are distorted and the ORL is thinned overlying drusen. It is noteworthy that CC perfusion did not appear to contribute to PL-BCVA measurements. For LL-BCVA, we found that the CC FD% parameter was included along with the OAC elevation volume and the ORL thickness measurements. This would suggest that as the CC FD% increases within the central macula, cone photoreceptor

function is further compromised, and this is evident from the LL-BCVA measurements. Thus, when the LLVAD score is calculated as the difference between the PL-BCVA and LL-BCVA scores, we find that the CC FD% plays a significant role in the magnitude of the LLVAD deficit score and its predictive value.

One possible scenario is that if the increase in CC FD%, which is observed in normal aging,[38] occurred in eyes genetically at-risk for developing AMD, then cone photoreceptor function would be significantly compromised in a dim light environment. However, if the CC FD% increased even more in eyes with AMD than would be expected in normal aging, then the low luminance visual function might be compromised to an even greater extent, and the impact of this increased CC FD% might result in an even greater LLVAD score. The only data that might support an increase in central CC FD% in eyes with AMD comes from the observation that there is a significant correlation between the drusen volume and CC FD% as shown not only in our current study, but also as previously reported by Nassisi *et al.*[39] Of note, unlike the previous report by Ou *et al.*[40], we did find a significant correlation between the drusen burden within both the central 1 mm and 3 mm regions of the macula and LLVAD measurements. We also found that the drusen volume within the central 1 mm and 3 mm regions correlated with an increase in the CC FD% measurements with both p-values less than 0.001 (data not shown). This circumstantial evidence could either support the notion that decreased CC perfusion drives drusen formation or drusen formation drives the decreased ability to detect CC perfusion. However, based on our previous study confirming our ability to detect CC FD% in the presence of large drusen,[41] it is unlikely that the presence of drusen compromised our ability to detect CC FD% using our current SS-OCTA based imaging strategy.

To test the hypothesis that there is a cause-and-effect relationship between CC perfusion and LL-BCVA, prospective studies will need to be performed in eyes with intermediate AMD to determine whether CC perfusion and LL-BCVA decreased over time in tandem or sequentially. If this cause-and-effect relationship were to be established, a study to test this relationship between CC perfusion and LL-BCVA might involve a targeted intervention that either increases CC perfusion and/or decreases damage to the photoreceptor/RPE complex. While complement inhibitors offer the best opportunity to prevent damage to the photoreceptor/RPE complex,[10,42] first an investigation on whether these drugs have any impact on CC perfusion is necessary to determine if photoreceptor/RPE damage drives the decrease in CC perfusion or whether the decrease in CC perfusion is independent of the photoreceptor/RPE damage. Another possible strategy would be to study the impact of CC perfusion alone on AMD by increasing perfusion to the choroid and CC by improving blood flow through the ophthalmic artery, either mechanically or pharmacologically. This could provide direct evidence to test whether CC perfusion plays a role in LL-BCVA and AMD progression.[43,44]

While rod-mediated dark adaptation at 5° eccentricity (RMDA 5°) test was shown to be a more sensitive indicator than LL-BCVA in separating normal eyes from intermediate AMD eyes,[45] a major advantage of using low luminance visual function tests in the study of AMD is that measuring LL-BCVA is simpler to perform and can be added onto routine ETDRS PL-BCVA testing. Moreover, low luminance testing measures the mesopic function of cone

photoreceptors and does not require dark adaptation. It is much faster to perform than other visual function tests, such as microperimetry, especially scotopic microperimetry,[46] and reading speed tests. However, low luminance testing only measures central cone photoreceptor function and has limited value once PL-BCVA drops below a Snellen equivalent of 20/50. Moreover, cataracts can significantly interfere with its measurement, therefore measurements in phakic eyes cannot be compared with those in pseudophakic eyes. Furthermore, if cataract surgery is performed during a prospective clinical trial, then the low luminance results will change unpredictably.[14]

The strength of our study is the analysis of clinically relevant macular structural parameters with SS-OCTA imaging that collectively powered our prediction models for the LLVAD scores even before the PL-BCVA was affected. The other strength is that the SS-OCTA measurements were performed on three repeated scans from each eye and then averaged, which increased the precision and reliability of our results. Major limitations include the relatively small number of subjects, Pearson correlations which did not account for the correlation between both eyes of subjects, and the lack of longitudinal follow-up. However, the significant correlations observed in this study should only be strengthened with greater numbers of subjects. The sensitivity analyses with the GEE models, which did account for the correlation between both eyes of subjects, produced similar results as the stepwise regressions. Additional imaging studies are underway to explain why eyes with nfGA appear to have worse low luminance cone function compared with drusen-only eyes at a given level of CC perfusion (Figure 3B). Several possibilities are being investigated; however, the most likely explanation is that there is an increase in basal laminar deposits,[47] which would only exacerbate the effects of decreased CC perfusion resulting in a further decrease in the nutritional support for the RPE and photoreceptors.[16,48] We also anticipate that additional parameters will need to be added to our current prediction models based on the departure from unity of our slope in Figure 4C. However, our goal in this study was to develop a prediction model using OCT parameters that can be reliably measured at this time from the same SS-OCTA scan.

In summary, the COMPARE study investigated the relationship between decreased central CC perfusion and increased LLVAD based on our hypothesis that the correlation between an increase in LLVAD scores and an increase in GA growth rates was mediated through an underlying decrease in CC perfusion. Our findings support our hypothesis and help explain how a foveal visual acuity test could predict the growth rate of nfGA when the atrophic lesion has not encroached on the fovea yet. In addition to central CC perfusion, the ORL thickness measurement was found to be a predictor of LLVAD. Our findings support a model that incorporates impairment of central CC perfusion and decrease in photoreceptor thickness as surrogate markers for cone visual dysfunction in eyes with and without neAMD.

ACKNOWLEDGEMENTS AND FINANCIAL DISCLOSURE:

Funding/Support:

Research supported by grants from Carl Zeiss Meditec, Inc., the Salah Foundation, an unrestricted grant from the Research to Prevent Blindness, Inc. (New York, NY), the National Eye Institute Center Core Grant (P30EY014801)

to the Department of Ophthalmology, University of Miami Miller School of Medicine, and grants from the National Eye Institute (R01EY028753). The funding organizations had no role in the design or conduct of the present research.

Financial Disclosures:

Philip Rosenfeld and Giovanni Gregori receive research support from Carl Zeiss Meditec, Inc. and the University of Miami co-own a patent that is licensed to Carl Zeiss Meditec, Inc.

Dr. Rosenfeld also received research funding from Gyroscope Therapeutics, Stealth BioTherapeutics, and Alexion Pharmaceuticals. He is also a consultant for Annexon, Apellis, Boehringer-Ingelheim, Carl Zeiss Meditec, Chengdu Kanghong Biotech, InflammX Therapeutics, Ocudyne, Regeneron Pharmaceuticals, and Unity Biotechnology. He also has equity interest in Apellis, Valitor, Verana Health, and Ocudyne.

Dr. Wang discloses intellectual property owned by the Oregon Health and Science University and the University of Washington. Dr. Wang also receives research support from Carl Zeiss Meditec Inc, Colgate Palmolive Company and Estee Lauder Inc. He is a consultant to Insight Photonic Solutions, Kowa, and Carl Zeiss Meditec and Cyberdontics.

Dr. Vanner receives research support from a Pediatric Glaucoma Research & Treatment Grant.

Dr. Qinqin Zhang and Dr. Luis de Sisternes are employees at Carl Zeiss Meditec, Inc.

The other authors have no disclosures.

Other Acknowledgments:

In memory of our beloved colleague, William J. Feuer, an extraordinary biostatistician and scientist. We appreciate the exceptional technical expertise of Linda O'Koren and Mark Lazcano in obtaining all the SS-OCT scans.

REFERENCES

1. Wood LJ, Jolly JK, Buckley TM, Josan AS, MacLaren RE. Low luminance visual acuity as a clinical measure and clinical trial outcome measure: a scoping review. Ophthalmic Physiol Opt. 2021;41(2):213–223. [PubMed: 33403668]
2. Sunness JS, Rubin GS, Broman A, Applegate CA, Bressler NM, Hawkins BS. Low luminance visual dysfunction as a predictor of subsequent visual acuity loss from geographic atrophy in age-related macular degeneration. Ophthalmology. 2008;115(9):1480–1488, 1488.e1481–1482. [PubMed: 18486216]
3. Sunness JS, Rubin GS, Applegate CA, et al. Visual function abnormalities and prognosis in eyes with age-related geographic atrophy of the macula and good visual acuity. Ophthalmology. 1997;104(10):1677–1691. [PubMed: 9331210]
4. Yehoshua Z, de Amorim Garcia Filho CA, Nunes RP, et al. Systemic complement inhibition with eculizumab for geographic atrophy in age-related macular degeneration: the COMPLETE study. Ophthalmology. 2014;121(3):693–701. [PubMed: 24289920]
5. Rosenfeld PJ, Berger B, Reichel E, et al. A Randomized Phase 2 Study of an Anti-Amyloid β Monoclonal Antibody in Geographic Atrophy Secondary to Age-Related Macular Degeneration. Ophthalmol Retina. 2018;2(10):1028–1040. [PubMed: 31047490]
6. Rosenfeld PJ, Dugel PU, Holz FG, et al. Emixustat Hydrochloride for Geographic Atrophy Secondary to Age-Related Macular Degeneration: A Randomized Clinical Trial. Ophthalmology. 2018;125(10):1556–1567. [PubMed: 29716784]
7. Holz FG, Sadda SR, Busbee B, et al. Efficacy and Safety of Lampalizumab for Geographic Atrophy Due to Age-Related Macular Degeneration: Chroma and Spectri Phase 3 Randomized Clinical Trials. JAMA Ophthalmol. 2018;136(6):666–677. [PubMed: 29801123]
8. Heier JS, Pieramici D, Chakravarthy U, et al. Visual Function Decline Resulting from Geographic Atrophy: Results from the Chroma and Spectri Phase 3 Trials. Ophthalmol Retina. 2020;4(7):673–688. [PubMed: 32199866]
9. Holekamp N, Wykoff CC, Schmitz-Valckenberg S, et al. Natural History of Geographic Atrophy Secondary to Age-Related Macular Degeneration: Results from the Prospective Proxima A and B Clinical Trials. Ophthalmology. 2020;127(6):769–783. [PubMed: 32081489]

10. Liao DS, Grossi FV, El Mehdi D, et al. Complement C3 Inhibitor Pegcetacoplan for Geographic Atrophy Secondary to Age-Related Macular Degeneration: A Randomized Phase 2 Trial. Ophthalmology. 2020;127(2):186–195. [PubMed: 31474439]
11. Steinle NC, Pearce I, Monés J, et al. Impact of Baseline Characteristics on Geographic Atrophy Progression in the FILLY Trial Evaluating the Complement C3 Inhibitor Pegcetacoplan. Am J Ophthalmol. 2021;227:116–124. [PubMed: 33675755]
12. Shi Y, Zhang Q, Zhou H, et al. Correlations Between Choriocapillaris and Choroidal Measurements and the Growth of Geographic Atrophy Using Swept Source OCT Imaging. Am J Ophthalmol. 2021;224:321–331. [PubMed: 33359715]
13. Wu Z, Guymer RH, Finger RP. Low luminance deficit and night vision symptoms in intermediate age-related macular degeneration. Br J Ophthalmol. 2016;100(3):395–398. [PubMed: 26250520]
14. Shen M, Shi Y, Wang L, et al. Impact of Cataract Surgery on Low Luminance Visual Acuity Deficit Measurements. Ophthalmology Science. 2022;2(3).
15. Jiang X, Shen M, Wang L, et al. Validation of a Novel Automated Algorithm to Measure Drusen Volume and Area Using Swept Source Optical Coherence Tomography Angiography. Transl Vis Sci Technol. 2021;10(4):11.
16. Chu Z, Shi Y, Zhou X, et al. Optical Coherence Tomography Measurements of the Retinal Pigment Epithelium to Bruch Membrane Thickness Around Geographic Atrophy Correlate With Growth. Am J Ophthalmol. 2022;236:249–260. [PubMed: 34780802]
17. Zhang Q, Shi Y, Shen M, et al. Does the Outer Retinal Thickness Around Geographic Atrophy Represent Another Clinical Biomarker for Predicting Growth? Am J Ophthalmol. 2022.
18. Shi Y, Yang J, Feuer W, Gregori G, Rosenfeld PJ. Persistent Hypertransmission Defects on En Face OCT Imaging as a Stand-Alone Precursor for the Future Formation of Geographic Atrophy. Ophthalmol Retina. 2021;5(12):1214–1225. [PubMed: 33610834]
19. Laiginhas R, Shi Y, Shen M, et al. Persistent Hypertransmission Defects Detected on En Face Swept Source Optical Computed Tomography Images Predict the Formation of Geographic Atrophy in Age-Related Macular Degeneration. Am J Ophthalmol. 2022;237:58–70. [PubMed: 34785169]
20. Liu J, Laiginhas R, Corvi F, et al. Diagnosing Persistent Hypertransmission Defects on En Face OCT Imaging of Age-Related Macular Degeneration. Ophthalmol Retina. 2022;6(5):387–397. [PubMed: 35093585]
21. Wang RK, An L, Francis P, Wilson DJ. Depth-resolved imaging of capillary networks in retina and choroid using ultrahigh sensitive optical microangiography. Opt Lett. 2010;35(9):1467–1469. [PubMed: 20436605]
22. Zhang A, Zhang Q, Chen CL, Wang RK. Methods and algorithms for optical coherence tomography-based angiography: a review and comparison. J Biomed Opt. 2015;20(10):100901.
23. Wu C. AI Quantification of OCTA en face image quality. Investigative Ophthalmology & Visual Science. 2019;60(11):PB099–PB099.
24. Haralick RM. Statistical and structural approaches to texture. Proceedings of the IEEE. 1979;67(5):786–804.
25. Tibshirani R. Regression Shrinkage and Selection Via the Lasso. Journal of the Royal Statistical Society: Series B (Methodological). 1996;58(1):267–288.
26. Garcia Filho CA, Yehoshua Z, Gregori G, et al. Change in drusen volume as a novel clinical trial endpoint for the study of complement inhibition in age-related macular degeneration. Ophthalmic Surg Lasers Imaging Retina. 2014;45(1):18–31. [PubMed: 24354307]
27. Chu Z, Gregori G, Rosenfeld PJ, Wang RK. Quantification of Choriocapillaris with Optical Coherence Tomography Angiography: A Comparison Study. Am J Ophthalmol. 2019;208:111–123. [PubMed: 31323202]
28. Zhang Q, Zhang A, Lee CS, et al. Projection artifact removal improves visualization and quantitation of macular neovascularization imaged by optical coherence tomography angiography. Ophthalmol Retina. 2017;1(2):124–136. [PubMed: 28584883]
29. Zhang Q, Shi Y, Zhou H, et al. Accurate estimation of choriocapillaris flow deficits beyond normal intercapillary spacing with swept source OCT angiography. Quant Imaging Med Surg. 2018;8(7):658–666. [PubMed: 30211033]

30. Zhang Q, Zheng F, Motulsky EH, et al. A Novel Strategy for Quantifying Choriocapillaris Flow Voids Using Swept-Source OCT Angiography. Invest Ophthalmol Vis Sci. 2018;59(1):203–211. [PubMed: 29340648]
31. Laiginhas R, Liu J, Shen M, et al. Multimodal Imaging, OCT B-Scan Localization, and En Face OCT Detection of Macular Hyperpigmentation in Eyes with Intermediate Age-Related Macular Degeneration. Ophthalmology Science. 2022;2(2):100116.
32. Zhang DQ, Chen SC. A novel kernelized fuzzy C-means algorithm with application in medical image segmentation. Artif Intell Med. 2004;32(1):37–50. [PubMed: 15350623]
33. Chu Z, Zhang Q, Gregori G, Rosenfeld PJ, Wang RK. Guidelines for Imaging the Choriocapillaris Using OCT Angiography. Am J Ophthalmol. 2021;222:92–101. [PubMed: 32891694]
34. Menghini M, Lujan BJ, Zayit-Soudry S, et al. Correlation of outer nuclear layer thickness with cone density values in patients with retinitis pigmentosa and healthy subjects. Invest Ophthalmol Vis Sci. 2014;56(1):372–381. [PubMed: 25515570]
35. Nunes RP, Gregori G, Yehoshua Z, et al. Predicting the progression of geographic atrophy in age-related macular degeneration with SD-OCT en face imaging of the outer retina. Ophthalmic Surg Lasers Imaging Retina. 2013;44(4):344–359. [PubMed: 23883530]
36. Bird AC, Phillips RL, Hageman GS. Geographic atrophy: a histopathological assessment. JAMA Ophthalmol. 2014;132(3):338–345. [PubMed: 24626824]
37. Riedl S, Vogl WD, Mai J, et al. The Effect of Pegcetacoplan Treatment on Photoreceptor Maintenance in Geographic Atrophy Monitored by Artificial Intelligence-Based OCT Analysis. Ophthalmol Retina. 2022.
38. Zheng F, Zhang Q, Shi Y, et al. Age-dependent Changes in the Macular Choriocapillaris of Normal Eyes Imaged With Swept-Source Optical Coherence Tomography Angiography. Am J Ophthalmol. 2019;200:110–122. [PubMed: 30639367]
39. Nassisi M, Tepelus T, Nittala MG, Sadda SR. Choriocapillaris flow impairment predicts the development and enlargement of drusen. Graefes Arch Clin Exp Ophthalmol. 2019;257(10):2079–2085. [PubMed: 31263948]
40. Ou WC, Denlar RA, Csaky KG. The Relationship Between Central Drusen Volume and Low-Luminance Deficit in Age-Related Macular Degeneration. Transl Vis Sci Technol. 2020;9(4):10.
41. Shi Y, Chu Z, Wang L, et al. Validation of a Compensation Strategy Used to Detect Choriocapillaris Flow Deficits Under Drusen With Swept Source OCT Angiography. Am J Ophthalmol. 2020;220:115–127. [PubMed: 32621895]
42. Jaffe GJ, Westby K, Csaky KG, et al. C5 Inhibitor Avacincaptad Pegol for Geographic Atrophy Due to Age-Related Macular Degeneration: A Randomized Pivotal Phase 2/3 Trial. Ophthalmology. 2021;128(4):576–586. [PubMed: 32882310]
43. Lylyk I, Bleise C, Lylyk PN, et al. Ophthalmic artery angioplasty for age-related macular degeneration. J Neurointerv Surg. 2022.
44. Rosenfeld PJ, Trivizki O, Gregori G, Wang RK. An Update on the Hemodynamic Model of Age-Related Macular Degeneration. Am J Ophthalmol. 2022;235:291–299. [PubMed: 34509436]
45. Owsley C, Swain TA, McGwin G Jr., et al. How Vision Is Impaired From Aging to Early and Intermediate Age-Related Macular Degeneration: Insights From ALSTAR2 Baseline. Transl Vis Sci Technol. 2022;11(7):17.
46. Nassisi M, Tepelus T, Corradetti G, Sadda SR. Relationship Between Choriocapillaris Flow and Scotopic Microperimetry in Early and Intermediate Age-related Macular Degeneration. Am J Ophthalmol. 2021;222:302–309. [PubMed: 32360341]
47. Sura AA, Chen L, Messinger JD, et al. Measuring the Contributions of Basal Laminar Deposit and Bruch's Membrane in Age-Related Macular Degeneration. Investigative Ophthalmology & Visual Science. 2020;61(13):19–19.
48. Iyer PG, Zhou H, Zhang Q, et al. Swept-Source Optical Coherence Tomography Detection of Bruch Membrane and Choriocapillaris Abnormalities in Sorsby Macular Dystrophy. Retina. 2022;42(9):1645–1654. [PubMed: 35483032]

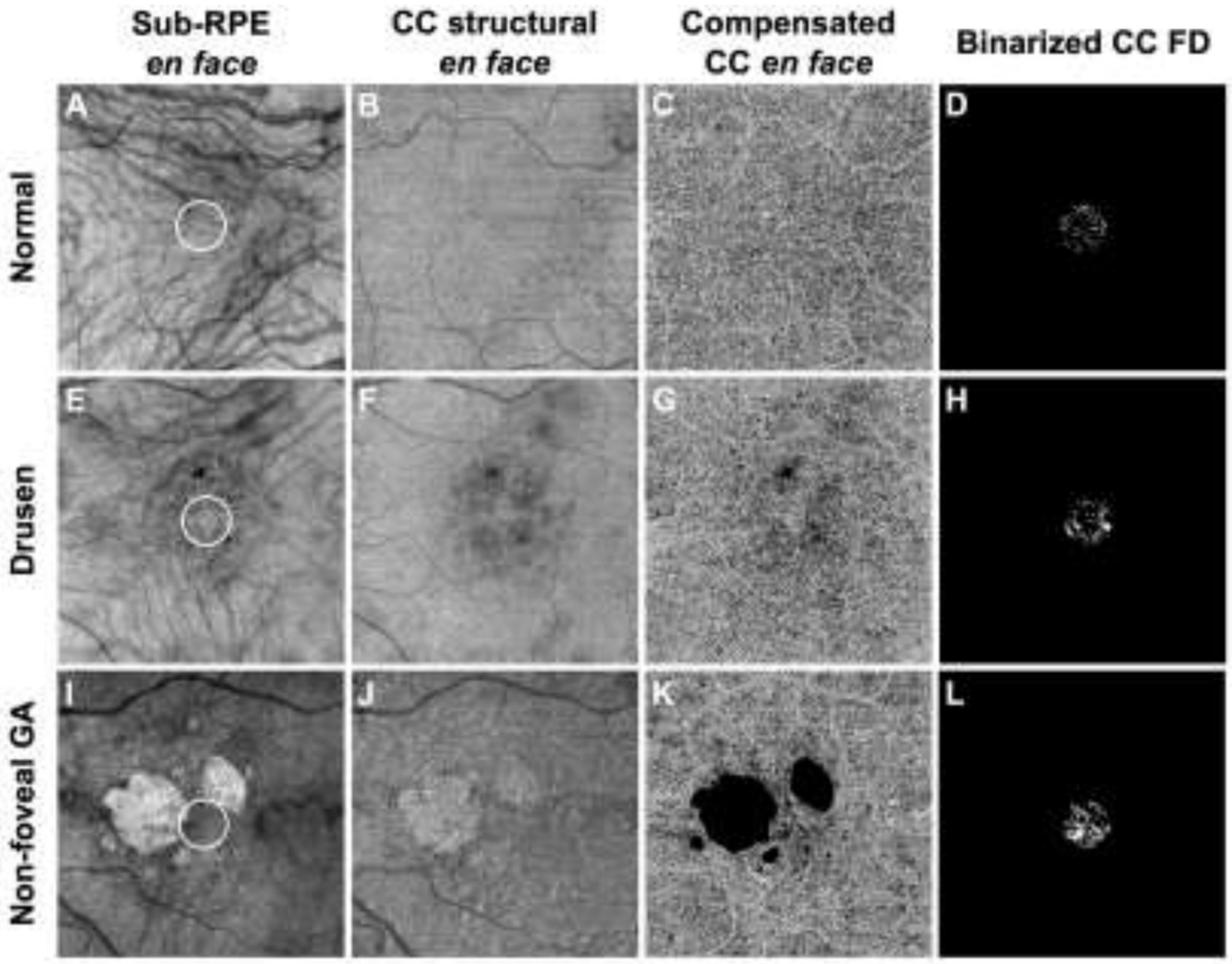

Figure 1:

Representative examples of a normal eye (A-D), a drusen-only eye (E-H) and an eye with non-foveal geographic atrophy (nfGA) (I-L) along with corresponding quantitation of choriocapillaris flow deficits (CC FDs). (A, E, I) Sub-RPE *en face* images showed evidence of hyperpigmentation in the drusen-only eye (E), and hypertransmission defects (hyperTDs) in the nfGA eye (I). The white 1 mm circle centered on the fovea indicates the area that was used to analyze the CC FDs. (B, F, J) CC structural *en face* images show a homogeneous area in normal eyes (B), areas with some shadowing from drusen and signal loss from hyperpigmentation (F), and areas with increased brightness corresponding to the persistent hypertransmission defect (hyperTD) (J). (C, G, K) Compensated CC angiographic *en face* images after excluding the hyperpigmentation and GA (black masks). (D, H, L) Binarized CC FD images were computed based on images C, G and K to measure the CC FD% in the central 1 mm circle (white foci denote the CC FDs).

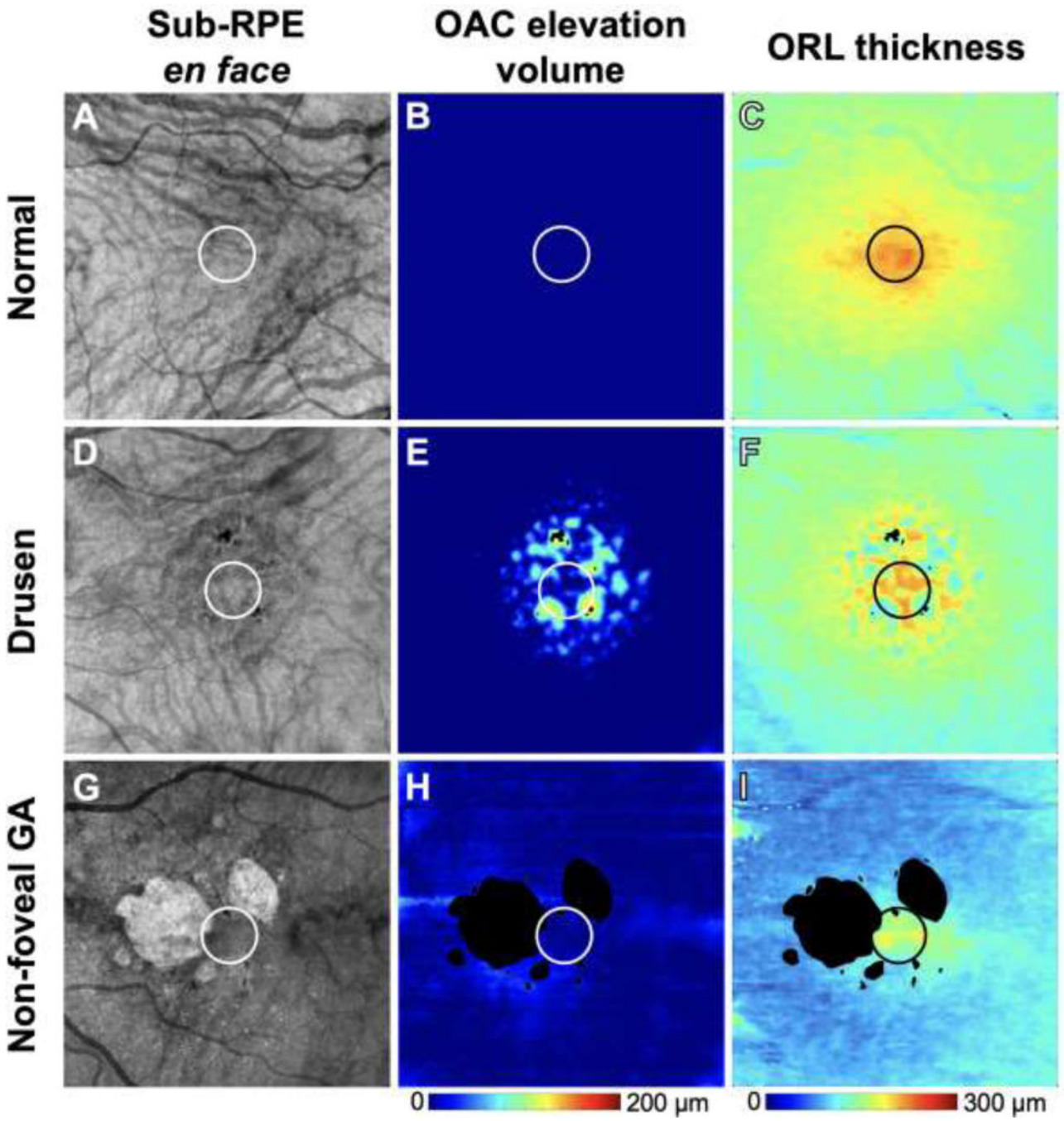

Figure 2:
The same representative examples as in Figure 1 of a normal eye (A-C), a drusen-only eye (D-F) and an eye with non-foveal geographic atrophy (G-I) along with corresponding measurements of optical attenuation coefficient (OAC) elevation volume (B, E, H) and outer retinal layer (ORL) thickness (C, F, I). The 1 mm circle centered on the fovea indicates the area that was used for quantification. Color bars: (B, E, H) OAC elevation volume: 0–200 µm; (C, F, I) ORL thickness: 0–300 µm.

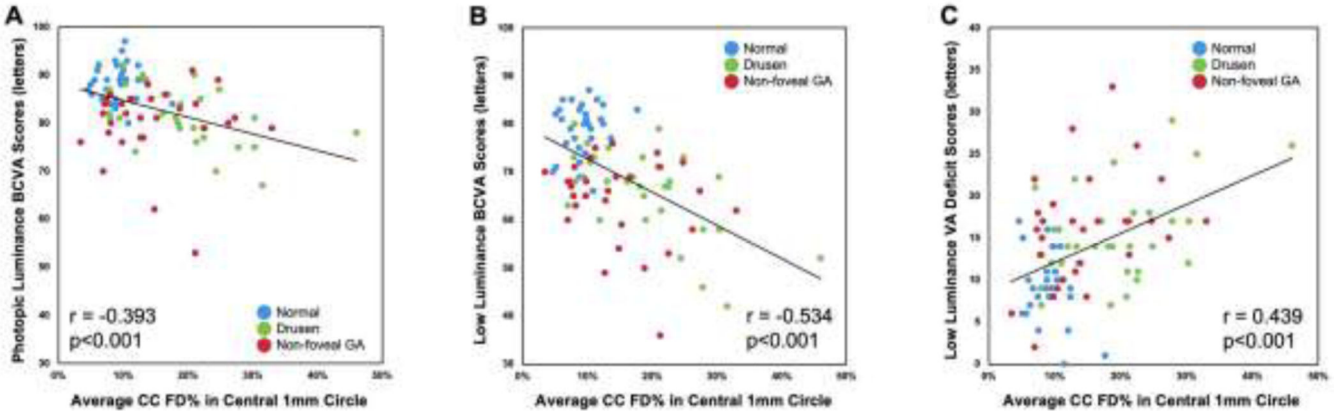

Figure 3:

Scatter plots showing correlations between choriocapillaris flow deficits percentages (CC FD%) in the central 1 mm circle and photopic luminance best-corrected visual acuity (PL-BCVA), low luminance BCVA (LL-BCVA) and low luminance visual acuity deficit (LLVAD) scores. In all 90 eyes (30 normal eyes; 31 drusen-only eyes; 29 eyes with non-foveal geographic atrophy), there were significant correlations between the CC FD% in central 1 mm circle and PL-BCVA ($r = -0.393$, $p<0.001$), LL-BCVA ($r = -0.534$, $p<0.001$), and LLVAD ($r = 0.439$, $p<0.001$).

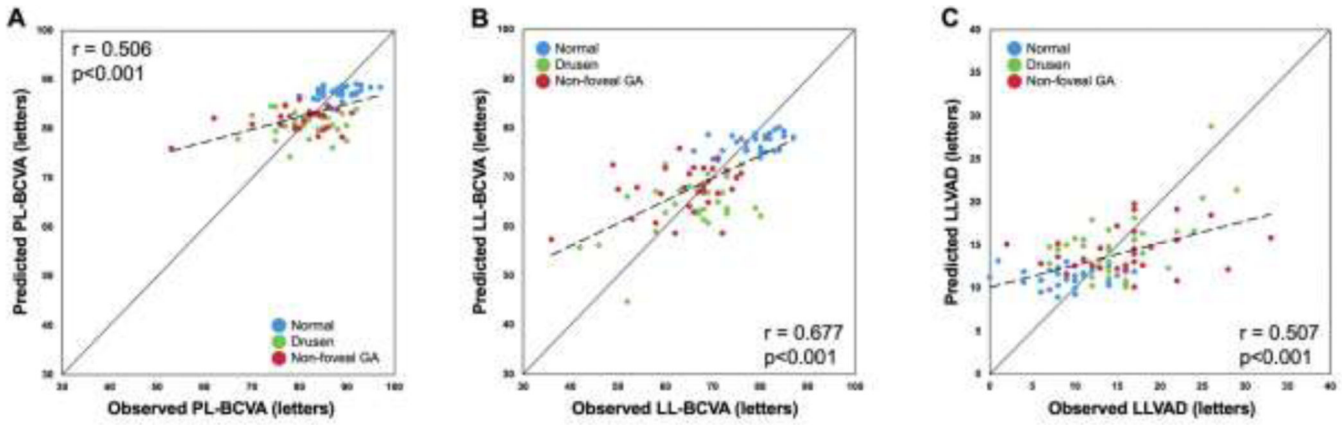

Figure 4:

Scatter plots of observed photopic luminance best-corrected visual acuity (PL-BCVA), low luminance BCVA (LL-BCVA) and low luminance visual acuity deficit (LLVAD) scores against the predicted PL-BCVA, LL-BCVA and LLVAD scores. The diagonal line is a 1:1 reference line. In all 90 eyes (30 normal eyes; 31 drusen-only eyes; 29 eyes with non-foveal geographic atrophy), there were significant correlations between the predicted and the observed PL-BCVA scores ($r= 0.506$, $p<0.001$), LL-BCVA scores ($r= 0.677$, $p<0.001$) and LLVAD scores ($r= 0.507$, $p<0.001$). The dashed line is a linear regression line.

Table 1:

Characteristics of eyes included in the COMPARE Study

	All (N=90)	Normal (N=30)	Drusen (N=31)	Non-foveal GA (N=29)	p value
Age, years, mean (SD)	74.17 (8.43)	66.11 (6.05)	76.81 (6.25)	79.67 (6.13)	**<0.001**
Gender, female (%)	59 (66%)	17 (57%)	23 (74%)	19 (66%)	=0.35
PL-BCVA scores, letters, mean (SD)	83.27 (7.02)	88.37 (3.86)	81.26 (6.00)	80.14 (7.77)	**<0.001**
LL-BCVA scores, letters, mean (SD)	69.69 (10.29)	78.93 (5.34)	65.90 (9.02)	64.17 (9.00)	**<0.001**
LLVAD scores, letters, mean (SD)	13.58 (6.22)	9.43 (4.21)	15.35 (5.54)	15.97 (6.63)	**<0.001**
CC FD% in central 1 mm circle, mean (SD)	14.36% (7.91%)	9.22% (2.84%)	19.03% (8.87%)	14.68% (7.34%)	**<0.001**
Cube root drusen volume in central 1 mm circle, mm, mean (SD)	0.13 (0.15)	0 (0)	0.26 (0.12)	0.13 (0.13)	**<0.001**
Cube root drusen volume in central 3 mm circle, mm, mean (SD)	0.25 (0.23)	0 (0)	0.43 (0.15)	0.30 (0.21)	**<0.001**
Cube root OAC elevation volume in central 1 mm circle, mm, mean (SD)	0.21 (0.13)	0.05 (0.04)	0.33 (0.07)	0.25 (0.08)	**<0.001**
ORL thickness in central 1 mm circle, μm, mean (SD)	184.70 (21.88)	198.27 (11.63)	179.06 (26.74)	176.68 (17.77)	**<0.001**

Abbreviations: GA=geographic atrophy; PL-BCVA=photopic luminance best-corrected visual acuity; LL-BCVA=low luminance best-corrected visual acuity; LLVAD=low luminance visual acuity deficit; CC FD=choriocapillaris flow deficit; OAC= optical attenuation coefficient; ORL=outer retinal layer; SD=standard deviation.

Table 2:

Correlations between OCT characteristics and PL-BCVA, LL-BCVA, LLVAD scores

	Age (years)	CC FD% in central 1 mm circle	Cube root drusen volume in central 1 mm circle (mm)	Cube root OAC elevation volume in central 1 mm circle (mm)	ORL thickness in central 1 mm circle (μm)
PL-BCVA	r= −0.321 **p=0.002**	r= −0.393 **p<0.001**	r= −0.334 **p=0.001**	r= −0.452 **p<0.001**	r= 0.375 **p<0.001**
LL-BCVA	r= −0.417 **p<0.001**	r= −0.534 **p<0.001**	r= −0.368 **p<0.001**	r= −0.538 **p< 0.001**	r= 0.522 **p<0.001**
LLVAD	r= 0.328 **p=0.002**	r= 0.439 **p<0.001**	r= 0.232 **p=0.028**	r= 0.380 **p<0.001**	r= −0.439 **p<0.001**

Abbreviations: OCT=optical coherence tomography; PL-BCVA=photopic luminance best-corrected visual acuity; LL-BCVA=low luminance best-corrected visual acuity; LLVAD=low luminance visual acuity deficit; CC FD=choriocapillaris flow deficit; OAC=optical attenuation coefficient; ORL=outer retinal layer.

Table 3:

Stepwise regression of the macular features correlated with the PL-BCVA, LL-BCVA, LLVAD scores

Parameters	PL-BCVA	LL-BCVA	LLVAD
Constant coefficient	72.85 **p<0.001**	56.15 **p<0.001**	25.64 **p<0.001**
CC FD% in central 1 mm circle	NA	−0.34 **p=0.009**	0.23 **p=0.007**
ORL thickness in central 1 mm circle (μm)	0.08 **p=0.016**	0.13 **p=0.004**	−0.08 **p=0.007**
Cube root OAC elevation volume in central 1 mm circle (μm)	−19.06 **p<0.001**	−25.39 **p<0.001**	NA

Abbreviations: PL-BCVA=photopic luminance best-corrected visual acuity; LL-BCVA=low luminance best-corrected visual acuity; LLVAD=low luminance visual acuity deficit; CC FD=choriocapillaris flow deficit; OAC= optical attenuation coefficient; ORL=outer retinal layer; NA=not applicable.